

SUPPLEMENTARY INFORMATION

Quasi-Enantiomeric Single-Nucleoside and Quasi-Racemic Two-Nucleosides Hydrochloride Salts and Ruthenium Complexes of Cytidine and 2',3'-Dideoxycytidine Analogs Unveiling the Negligible Structure-Driving Role of the 2',3'-Moieties

Felipe Terra Martins,^{a,} Rodrigo S. Corrêa,^b Alzir Azevedo Batista,^b Javier Ellena^c*

^a*Instituto de Química, Universidade Federal de Goiás, Campus Samambaia, CP 131, 74001-970, Goiânia, GO, Brazil;*

^b*Departamento de Química, Universidade Federal de São Carlos – UFSCar, Rodovia Washington Luís KM 235, CP 676, 13561-901, São Carlos, SP, Brazil;* ^c*Departamento de Física e Informática, Instituto de Física de São Carlos, Universidade de São Paulo, CP 369, 13560-970, São Carlos, SP, Brazil* * To whom correspondence should be addressed. E-mail:

felipe@ufg.br

Content:

Tables S1 (crystal data for **2-5**), S2 (main torsion angles and planarity descriptors for **1-3**), S3 (hydrogen bond table for **2** and **3**), S4 (main bond angles and lengths for **4** and **5**), S5 (main torsion angles for **4** and **5**), and S6 (hydrogen bond table for **4** and **5**), Figures S1 (complete geometry for stacking interactions in **1-3**), S2, S3 (ellipsoid plots for **4** and **5**), S4 to S10 (NMR experiments for **4** and **5**), S11, S12 (electrochemical experiments for **4** and **5**), S13 and S14 (infrared spectra for **4** and **5**)

Table S1 - Crystal data and refinement statistics for the multicomponent molecular forms [zalcitabine hydrochloride (**2**) and lamivudine zalcitabine hydrochloride (**3**)] and ruthenium(II) complexes {*trans*-[Ru(PPh₃)₂(3TC)(bipy)]ClO₄ (**4**) and *trans*-[Ru(PPh₃)₂(CYD)(bipy)]ClO₄ (**5**)} prepared in this study.

		2		3		4		5	
structural formula		(C ₉ H ₁₄ N ₃ O ₃)Cl		(C ₉ H ₁₄ N ₃ O ₃)(C ₈ H ₁₂ N ₃ O ₃ S)2Cl		[RuC ₅₄ H ₄₉ N ₅ O ₂ P ₂ S].ClO ₄ .H ₂ O. (CH ₃) ₂ CO		2[RuC ₅₅ H ₅₀ N ₅ O ₅ P ₂].(ClO ₄) ₂ . 1½H ₂ O.½CH ₃ OH.(CH ₃ CH ₂) ₂ O	
fw (g/mol)		247.68		513.40		1185.59		2364.08	
cryst dimensions (mm ³)		0.60 x 0.12 x 0.06		0.13 x 0.11 x 0.09		0.18 x 0.08 x 0.07		0.31 x 0.11 x 0.05	
cryst syst		monoclinic		triclinic		orthorhombic		monoclinic	
space group		P2 ₁		P1		P2 ₁ 2 ₁ 2 ₁		P2 ₁	
Z/Z'		2 / 1		2 / 2		4/4		2/4	
T (K)		298(2)		298(2)		293(2)		293(2)	
unit cell dimensions									
	<i>a</i> (Å)	5.5482(2)	5.467 (2)	6.706(3)	6.692(1)	9.800(5)	10.432(1)	10.432(1)	10.432(1)
	<i>b</i> (Å)	12.0260(5)	11.978 (3)	9.155(8)	8.886(1)	16.008(5)	20.600(3)	20.600(3)	20.600(3)
	<i>c</i> (Å)	8.5725(3)	8.540(2)	10.512(7)	10.412(1)	34.268(5)	27.012(5)	27.012(5)	27.012(5)
	α (°)	90	90	105.81(2)	105.22(1)	90	90	90	90
	β (°)	104.639(2)	105.327(2)	98.48(1)	99.04(1)	90	98.20(5)	98.20(5)	98.20(5)
	γ (°)	90	90	108.40(2)	107.50(1)	90	90	90	90
<i>V</i> (Å ³)		553.41(4)		569.6(7)		5376(3)		5745.5(1)	
calculated density (Mg/m ³)		1.486		1.497		1.465		1.367	
<i>Refinement (only on low temp. data)</i>									
absorption coefficient μ (mm ⁻¹)		0.342		0.351		0.438		0.437	
Transmission factors for absorption correction (Gaussian)		<i>T</i> _{min} = 0.882	<i>T</i> _{min} = 0.860	<i>T</i> _{min} = 0.959	<i>T</i> _{min} = 0.937	<i>T</i> _{min} = 0.971	<i>T</i> _{min} = 0.906	<i>T</i> _{min} = 0.906	<i>T</i> _{min} = 0.906
		<i>T</i> _{max} = 0.981	<i>T</i> _{max} = 0.980	<i>T</i> _{max} = 0.985	<i>T</i> _{max} = 0.971	<i>T</i> _{max} = 0.971	<i>T</i> _{max} = 0.972	<i>T</i> _{max} = 0.972	<i>T</i> _{max} = 0.972
θ range for data collection (°)		3.97 – 24.85		3.30-25.11		3.02 to 25.25		3.02 to 26.38	
index ranges									
	<i>h</i>	-6 to 6		-7 to 7		-11 to 11		-13 to 13	
	<i>k</i>	-13 to 13		-10 to 10		-19 to 18		-25 to 25	
	<i>l</i>	-9 to 9		-11 to 10		-41 to 33		-33 to 33	
data collected		4896		7307		24783		44046	
unique reflections		1653		3091		9650		22785	
symmetry factor (<i>R</i> _{int})		0.0655		0.0517		0.0884		0.0380	
completeness to θ _{max} (%)		97.1		99.5		99.2		99.5	
<i>F</i> (000)		260		268		2448		2444	
parameters refined		157		232		686		1414	
goodness-of-fit on <i>F</i> ²		1.074		1.099		0.999		1.004	
final <i>R</i> factors for <i>I</i> > 2 σ (<i>I</i>)		<i>R</i> ₁ = 0.0407	<i>R</i> ₁ = 0.0403	<i>R</i> ₁ = 0.0656	<i>R</i> ₁ = 0.0657	<i>R</i> ₁ = 0.0657	<i>R</i> ₁ = 0.0470	<i>R</i> ₁ = 0.0470	<i>R</i> ₁ = 0.0470
		<i>wR</i> ₂ = 0.1048	<i>wR</i> ₂ = 0.1035	<i>wR</i> ₂ = 0.1453	<i>wR</i> ₂ = 0.1443	<i>wR</i> ₂ = 0.1443	<i>wR</i> ₂ = 0.1081	<i>wR</i> ₂ = 0.1081	<i>wR</i> ₂ = 0.1081

<i>R</i> factors for all data		<i>RI</i> = 0.0440	<i>RI</i> = 0.0413	<i>RI</i> = 0.0792	<i>R</i> 1 = 0.0963	<i>R</i> 1 = 0.0768
		<i>wR</i> 2 = 0.1083	<i>wR</i> 2 = 0.1053	<i>wR</i> 2 = 0.1558	<i>wR</i> 2 = 0.1560	<i>wR</i> 2 = 0.1184
largest diff. peak / hole ($e/\text{\AA}^3$)		0.380/-0.160	0.246/-0.338	0.391/-0.369	2.476 and -0.533	1.026 and -0.418
absolute structure	Flack parameter	0.05(9)	-0.02(7)	0.03(16)	0.05(4)	0.09(2)
	Friedel pairs	779	1054	1408	4256	10747
CCDC deposit number		788023	788024	787748	976187	976188

Table S2 - Selected Torsion Angles (deg.) for the conformationally variable structure moieties of lamivudine and zalcitabine and descriptors for planarity between cytosine and chloride (r.m.s. deviation and chloride deviation in Å) in the single-drug hydrochloride salts (**1**¹² and **2**) and in the two-drugs one (**3**) determined by single-crystal X-ray diffraction data at 150 K.

Structure moiety	Torsion	1	2	3	
				zalcitabine	lamivudine
N1—C1' bridge between cytosine and the five- membered rings	C2—N1—C1'—O1'	161.9(2)	-162.5(2)	-165.3(8)	158.6(8)
	C6—N1—C1'—O1'	-22.1(3)	17.9(3)	22(1)	-27(1)
	C2—N1—C1'—C2'	-78.1(3)	79.7(2)	77(1)	-83(1)
	C6—N1—C1'—C2'	97.9(3)	-99.8(2)	-96(1)	91(1)
Five-membered ring	O1'—C1'—C2'—C3'(S3')	35.4(4)	-25.8(2)	-28.8(9)	33.5(8)
	C1'—C2'—C3'(S3')—C4'	-41.4(3)	35.8(2)	37.3(9)	-41.9(7)
	C2'—C3'(S3')—C4'—O1'	38.7(3)	-34.1(2)	-35.7(9)	40.2(7)
	C3'(S3')—C4'—O1'—C1'	-24.8(4)	19.1(2)	19(1)	-27.5(9)
	C4'—O1'—C1'—C2'	-6.6(5)	4.6(2)	7(1)	-4(1)
5'-CH ₂ OH branch	O1'—C4'—C5'—O5'	-175.8(2)	172.5(2)	60(1)	-142(2) ^[a] / -75(2) ^[b]
	C3'(S3')—C4'—C5'—O5'	65.1(3)	-69.2(3)	-174.8(8)	71(1) ^[a] / 165(2) ^[b]
cytosine least-square (l.s.) plane	N1—C2—O2—N3—C4—N4—C5—C6 r.m.s.d.	0.0310	0.0172	0.0720	0.0721
chloride-cytosine coplanarity	Cl ^[c] deviation from the cytosine l.s. plane	0.092(1)	0.079(1)	0.144(2)	0.059(3)
	Cl ^[d] deviation from the cytosine l.s. plane	1.434(1)	1.673(1)	0.052(2)	0.172(3)

^[a] The fractions of the C5' and O5' atoms are in the major 60% occupancy sites. ^[b] The fractions of the C5' and O5' atoms are in the minor 40% occupancy sites. ^[c] Chloride counterion held together through two hydrogen bonds in which protonated cytosine ring of the drugs is a donor through its imine and amine moieties. ^[d] Chloride counterion involved in just one hydrogen bonding in which amine moiety is donor through its hydrogen opposite to imine moiety.

Table S3 - Intermolecular hydrogen bonding geometry of the multicomponent molecular forms prepared in this study at low temperature (150 K).

D—H•••R	D—H (Å)	H•••R (Å)	D•••R (Å)	D—H•••R (°)
2				
N ₃ ⁽⁺⁾ —H ₃ •••Cl ₁ ⁽⁻⁾	0.90(3)	2.19(3)	3.047(2)	159(3)
N ₄ —H _{4Nx} •••Cl ₁ ⁽⁻⁾	1.05(3)	2.38(3)	3.343(2)	152(3)
N ₄ —H _{4Ny} •••Cl ₁ ⁽⁻⁾ [a]	0.89(3)	2.44(3)	3.259(2)	152(3)
O ₅ '—H _{5'O} •••O ₂ ^[b]	0.82(3)	1.94(3)	2.734(3)	163(3)
3				
N _{3L} ⁽⁺⁾ —H _{3L} •••Cl ₁ ⁽⁻⁾	0.86	2.22	3.057(9)	164
N _{4L} —H _{4NxL} •••Cl ₁ ⁽⁻⁾	0.86	2.63	3.379(9)	146
N _{4L} —H _{4NyL} •••Cl ₁ ⁽⁻⁾ [c]	0.86	2.58	3.385(9)	157
N _{3Z} ⁽⁺⁾ —H _{3Z} •••Cl ₂ ⁽⁻⁾	0.86	2.28	3.118(9)	164
N _{4Z} —H _{4NxZ} •••Cl ₂ ⁽⁻⁾	0.86	2.65	3.393(9)	146
N _{4Z} —H _{4NyZ} •••Cl ₂ ⁽⁻⁾ [d]	0.86	2.57	3.382(9)	159
O _{5'L} —H _{5'OL} •••O _{5'Z} ^[e]	0.82	2.09	2.77(1)	140
O _{5'L} '—H _{5'OL} '•••Cl ₂ ⁽⁻⁾	0.82	2.34	3.11(1)	158
O _{5'Z} '—H _{5'OZ} '•••Cl ₁ ⁽⁻⁾	0.82	2.46	3.114(7)	134

Symmetry operators: [a] - 1 - x; 0,5 + y; 1 - z; [b] - x; 0,5 + y; - z; [c] 1 + x; y; z; [d] - 1 + x; y; z; [e] 1 + x; 1 + y; - 1 + z.

Table S4 - Selected bond and angle lengths (Å, °) for [Ru(PPh₃)₂(3TC)(bipy)]ClO₄ and [Ru(PPh₃)₂(CYD)(bipy)]ClO₄ around the metal center and the main bond lengths of the cytosine ring and five-membered ring.

Fragment	4	5	
		<i>Molecule A</i>	<i>Molecule B</i>
Metal center			
d Ru1—N3	2.165(5)	2.122(6)	2.128(5)
d Ru1—N4	2.150(6)	2.146(5)	2.129(4)
d Ru1—N2	2.071(6)	2.060(5)	2.071(5)
d Ru1—N5	2.039(6)	2.044(5)	2.055(5)
d Ru1—P1	2.387(2)	2.389(2)	2.384(2)
d Ru1—P2	2.396(2)	2.403(2)	2.401(2)
< N3—Ru1—N4	61.3(2)	61.5(2)	61.18(19)
< N2—Ru1—N5	77.2(2)	78.3(2)	77.0(2)
< P1—Ru1—P2	179.43(7)	176.13(6)	176.46(6)
< N2—Ru1—N3	172.0(2)	171.7(2)	173.7(2)
< N2—Ru1—N4	110.7(2)	110.3(2)	112.5(2)
< N3—Ru1—N5	110.8(2)	109.9(2)	109.2(2)
< P1—Ru1—N3	88.4(2)	88.69(16)	88.90(15)
< P1—Ru1—N4	87.5(1)	89.67(16)	87.67(16)
< P2—Ru1—N3	91.8(2)	87.54(16)	87.78(15)
< P2—Ru1—N4	92.1(2)	87.77(16)	89.66(16)
Cytosine ring			
d C2—O2	1.238(8)	1.285(8)	1.198(8)
d C4—N4	1.324(9)	1.302(8)	1.305(7)
d C4—N3	1.360(9)	1.378(8)	1.370(8)
d C2—N3	1.346(9)	1.334(8)	1.360(8)
d C2—N1	1.427(9)	1.393(9)	1.410(8)
d N1—C6	1.378(10)	1.358(10)	1.391(9)
d C5—C6	1.335(11)	1.276(10)	1.377(9)
d C5—C4	1.444(10)	1.437(8)	1.429(8)
Five-membered ring			
d N1—C1'	1.463(9)	1.524(8)	1.444(8)
d C1'—O1'	1.430(9)	1.418(8)	1.382(7)
d C1'—C2'	1.483(11)	1.479(9)	1.483(10)
d O1'—C4'	1.442(9)	1.422(9)	1.459(7)
d C4'—S3'(C3')	1.840(8)	1.514(12)	1.510(11)
d C2'—S3'(C3')	1.817(8)	1.529(9)	1.516(13)

Table S5 - Selected Torsion Angles (deg.) for the conformationally variable structure moieties of lamivudine and cytidine into ruthenium complexes.

Structure moiety	Torsion	4	5	
			cytidine A	cytidine B
N1—C1' bridge between cytosine and the five- membered rings	C2—N1—C1'—O1'	120.9(7)	-150.1(6)	-159.1(6)
	C6—N1—C1'—O1'	-54.9(9)	29.6(10)	5.5(10)
	C2—N1—C1'—C2'	-120.1(8)	93.3(8)	79.9(9)
	C6—N1—C1'—C2'	64.1(10)	-87.0(10)	-115.6(8)
Five-membered ring	O1'—C1'—C2'—C3'(S3')	-43.5(8)	38.3(8)	-28.6(9)
	C1'—C2'—C3'(S3')—C4'	-25.8(6)	-22.4(10)	38.3(9)
	C2'—C3'(S3')—C4'—O1'	-3.6(6)	-0.1(12)	-34.7(9)
	C3'(S3')—C4'—O1'—C1'	-21.4(8)	23.3(12)	19.1(9)
	C4'—O1'—C1'—C2'	43.2(9)	-38.2(9)	6.0(8)
5'-CH ₂ OH branch	O1'—C4'—C5'—O5'	-66.7(9)	-62.5(17)	-64.6(13)
	C3'(S3')—C4'—C5'—O5'	-53.7(9)	58.5(16)	54.9(15)

Table S6 – Main intermolecular hydrogen bonding geometry of the metal complexes.

D—H•••R	D—H (Å)	H•••R (Å)	D•••R (Å)	D—H•••R (°)
4				
N ₄ —H ₄ •••O _{1s} ^[a]	0.86	2.73	3.533(11)	155
O _{1w} —H _{1w} •••O ₅ ' ^[b]	0.85	2.02	2.844(10)	162
O _{1w} —H _{2w} •••O ₂	0.85	2.21	2.919(9)	141
5				
N ₄ —H ₄ •••O _{2s}	0.86	2.43	3.236(11)	157
N _{4A} —H _{4A} •••O _{7s} ^[c]	0.86	2.53	3.332(10)	156
O _{1w} —H _{12w} •••O ₅ '' ^[d]	0.85	2.27	3.114(16)	175
O _{3wa} —H _{23a} •••O ₂ ' ^[e]	0.85	2.13	2.90(2)	149

Symmetry operators: ^[a] x,+y-1,+z; ^[b] 1+x,y,z; ^[c] -1+x,y,z; ^[d] -x, -1/2+y,1-z; ^[e] -x, 1/2+y,-z.

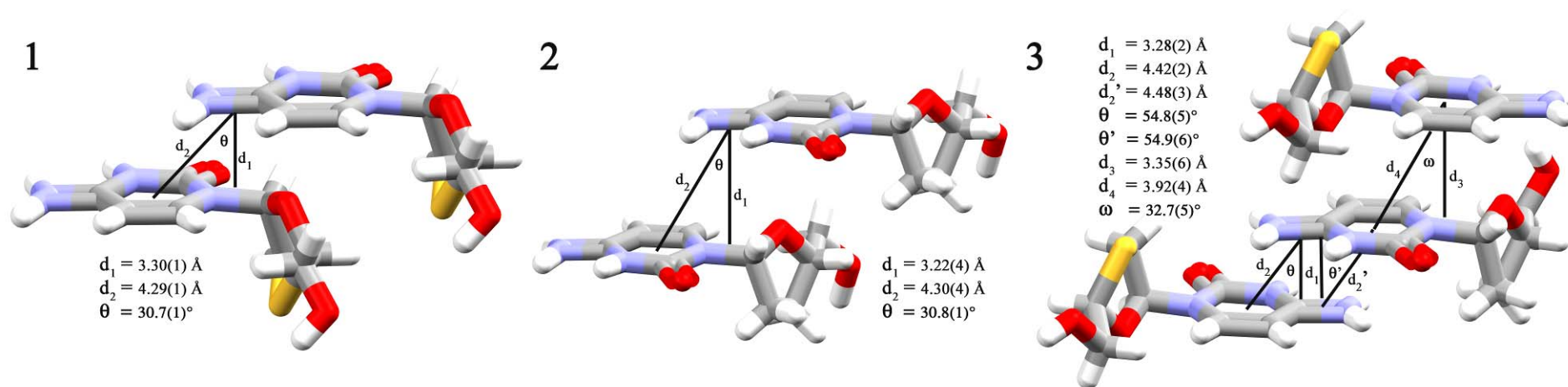


Figure S1- Complete geometry of the π - π base-stacking interactions in the hydrochloride salts **1-3** determined by single-crystal X-ray diffraction data at 150 K. The distance d_1 was calculated between the cytosine least-square (l.s.) planes (see Table S2 for plane definition and r.m.s. deviation). The distance d_2 , as well as d_2' , was calculated between two centroids, namely, that between C4 and N4 and that among the N1—C2—N3—C4—C5—C6 atoms. The distance d_3 was calculated between the cytosine least-square (l.s.) planes of lamivudine and zalcitabine (see Table S2 for planes definition and r.m.s. deviation), while d_4 is the distance between the centroids among the N1—C2—N3—C4—C5—C6 atoms.

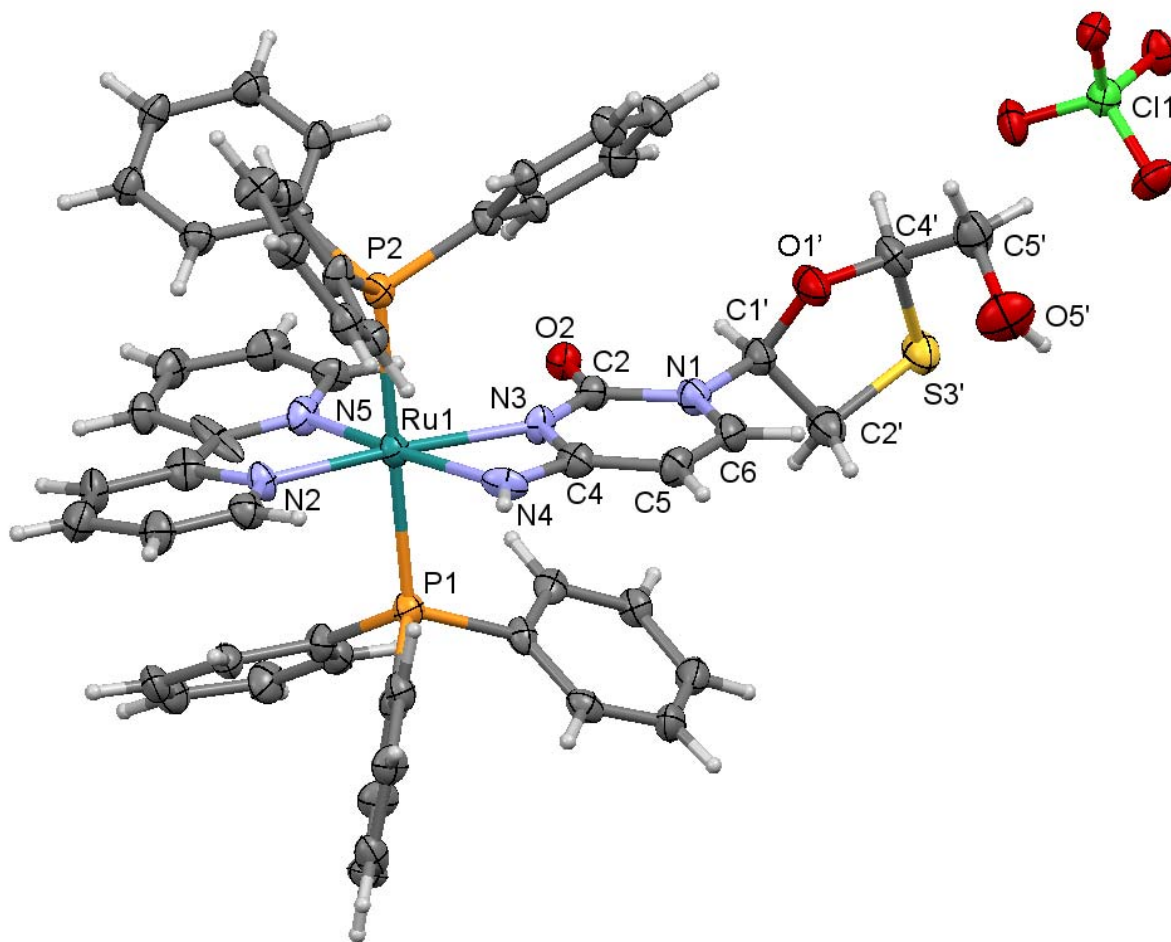


Figure S2- 30% Probability ellipsoids drawing for non-hydrogen atoms of *trans*-[Ru(PPh₃)₂(3TC)(bipy)]ClO₄.

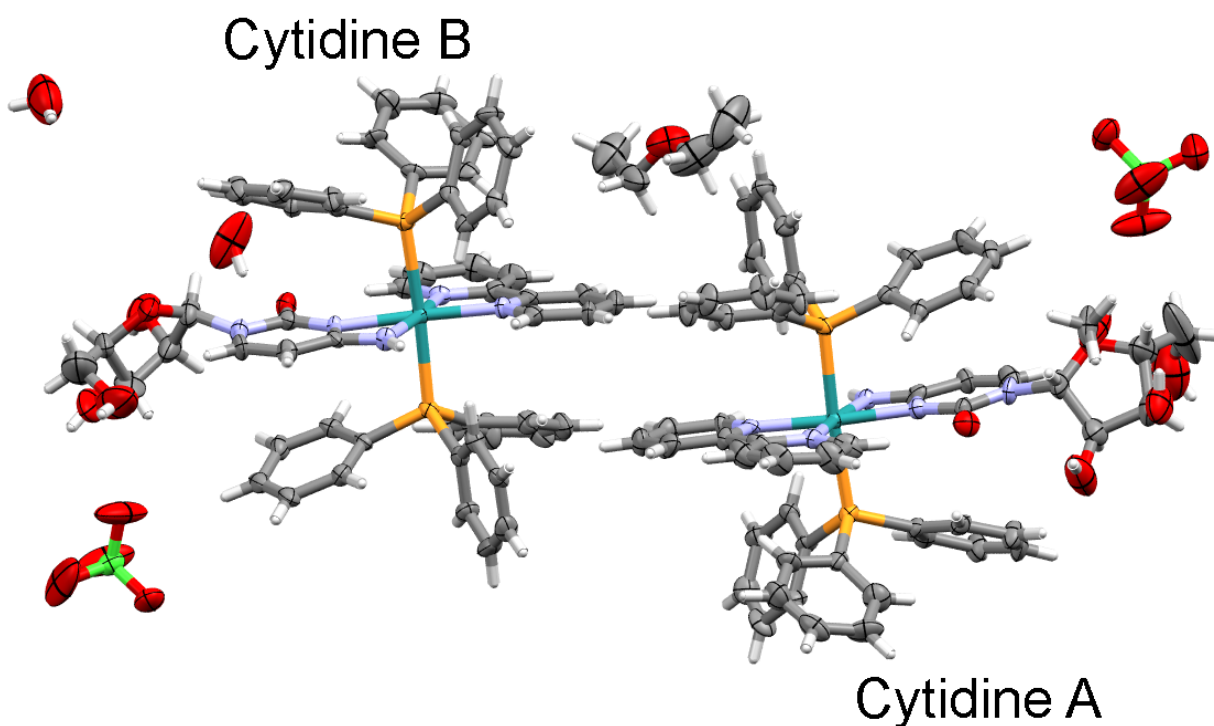


Figure S3 - 30% Probability ellipsoids drawing for non-hydrogen atoms of *trans*-[Ru(PPh₃)₂(CYD)(bipy)]ClO₄.

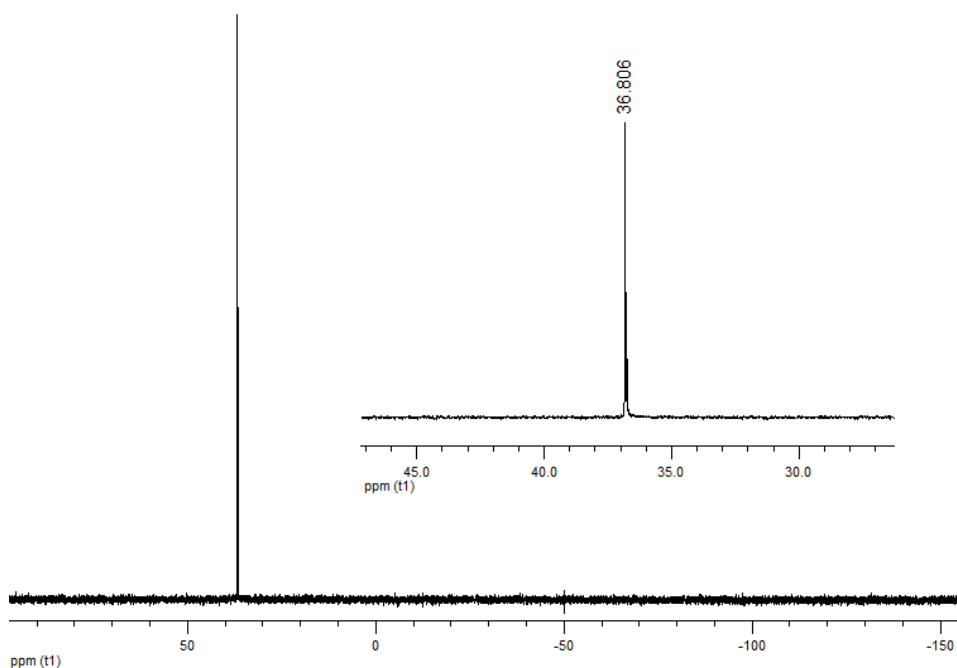


Figure S4 - ^{31}P NMR spectrum for *trans*-[Ru(PPh₃)₂(3TC)(bipy)]ClO₄, in CDCl₃.

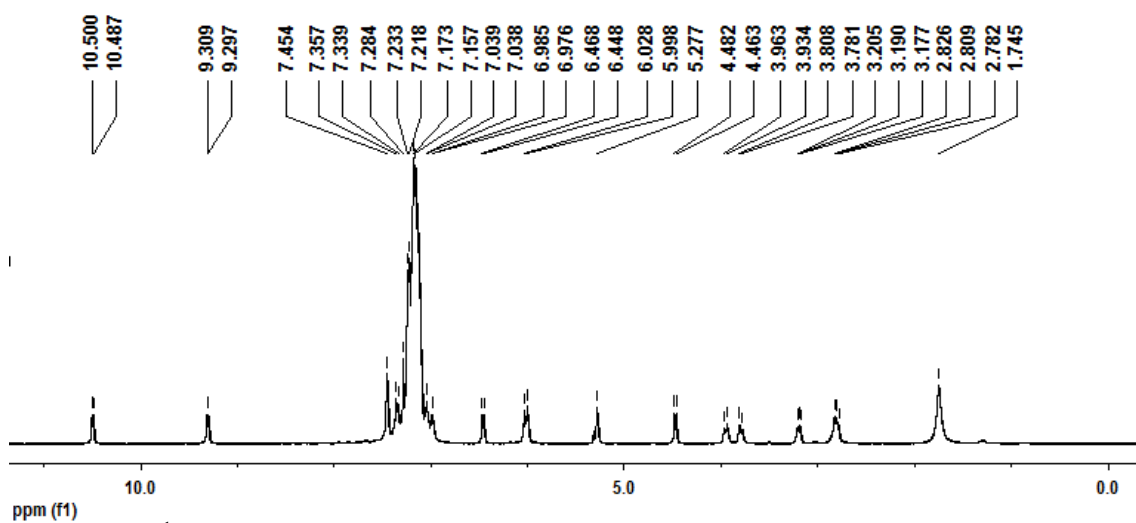


Figure S5 - ^1H NMR spectrum for *trans*-[Ru(PPh₃)₂(3TC)(bipy)]ClO₄, in CDCl₃.

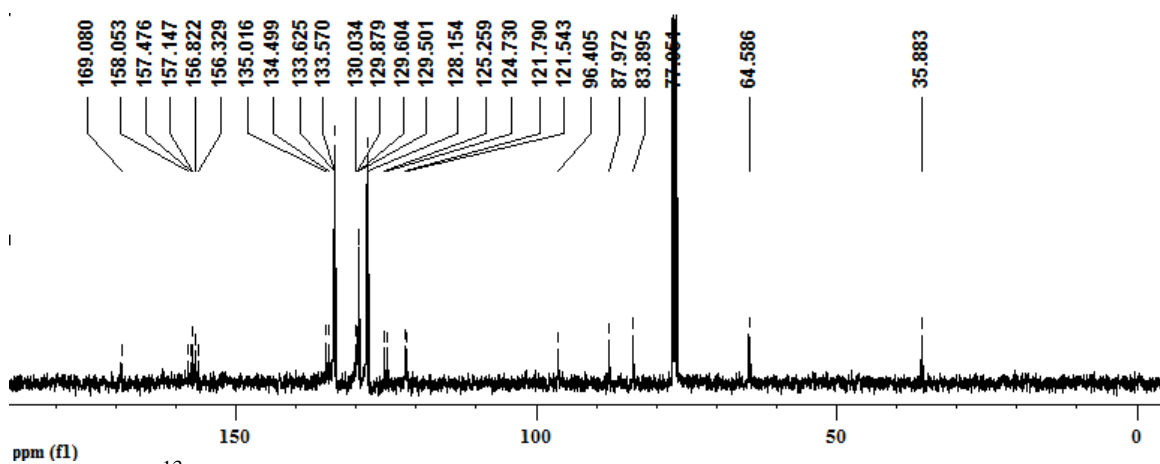


Figure S6 - ^{13}C NMR spectrum for *trans*-[Ru(PPh₃)₂(3TC)(bipy)]ClO₄, in CDCl₃.

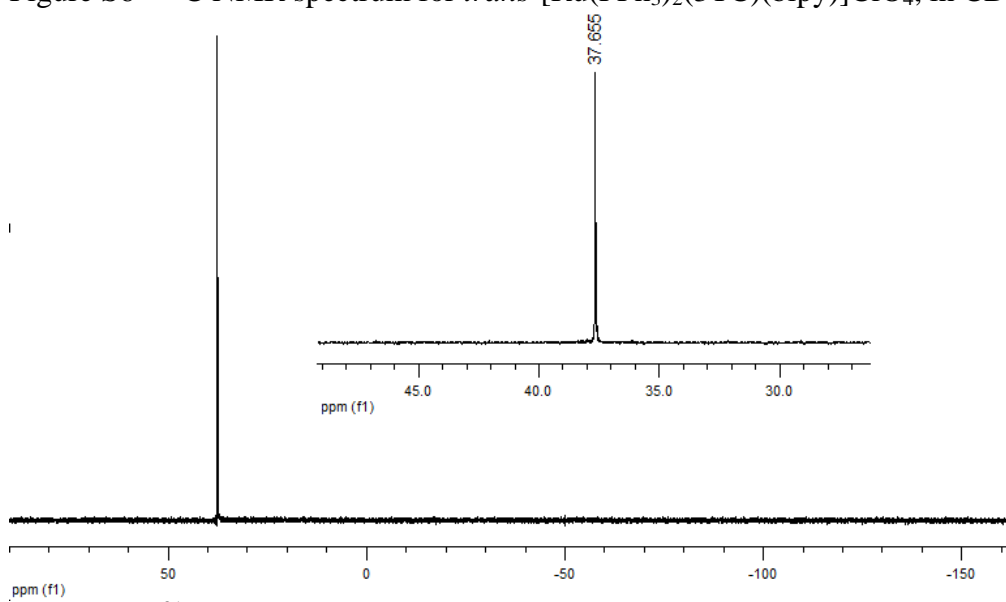


Figure S7 - ^{31}P NMR spectrum for *trans*-[Ru(PPh₃)₂(CYD)(bipy)]ClO₄, in CDCl₃.

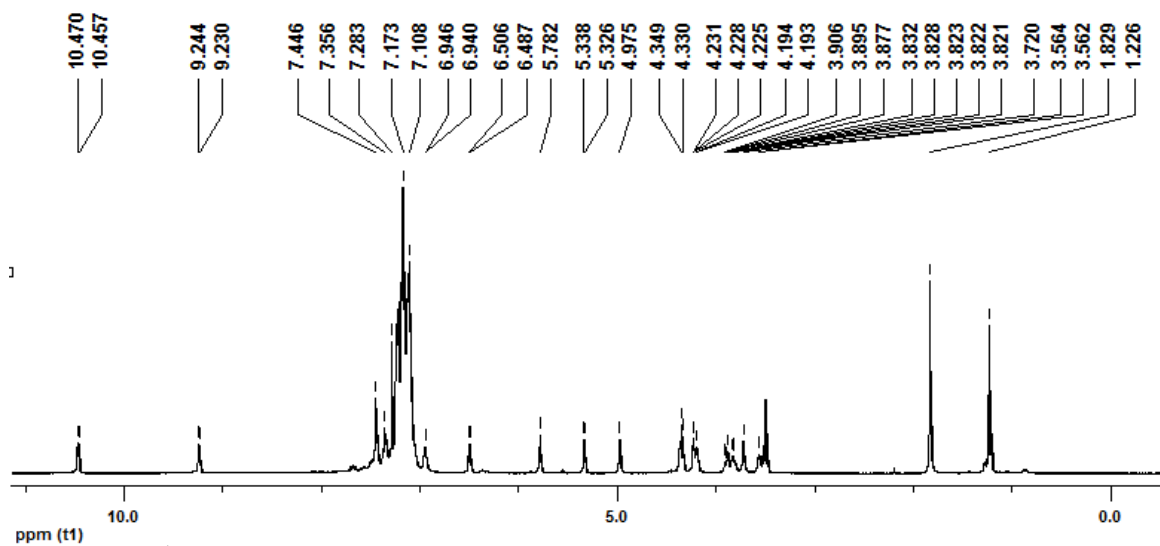


Figure S8 - ^1H NMR spectrum for *trans*-[Ru(PPh₃)₂(CYD)(bipy)]ClO₄, in CDCl₃.

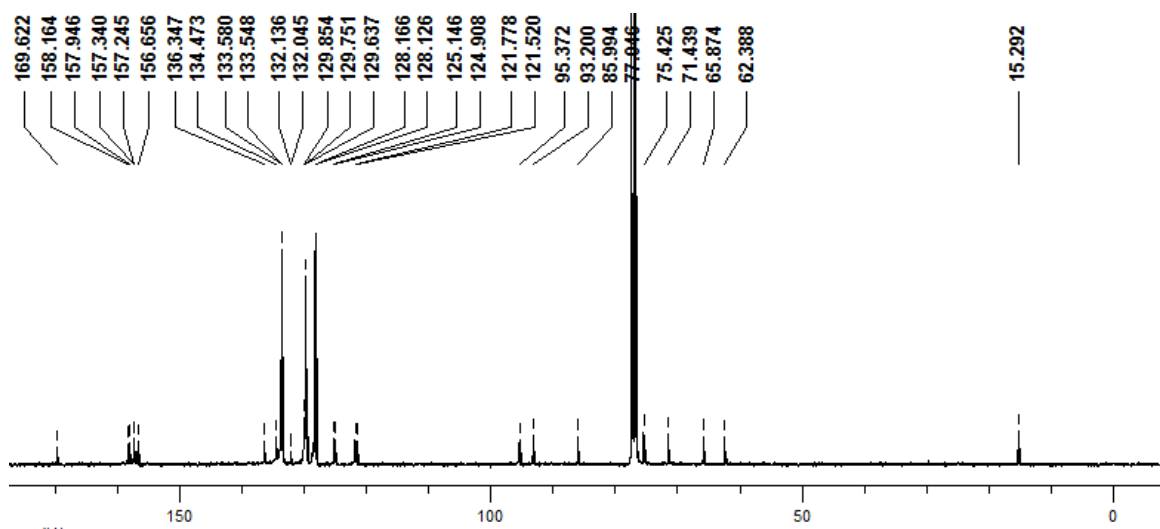


Figure S9 - ^{13}C NMR spectrum for *trans*-[Ru(PPh₃)₂(CYD)(bipy)]ClO₄, in CDCl₃.

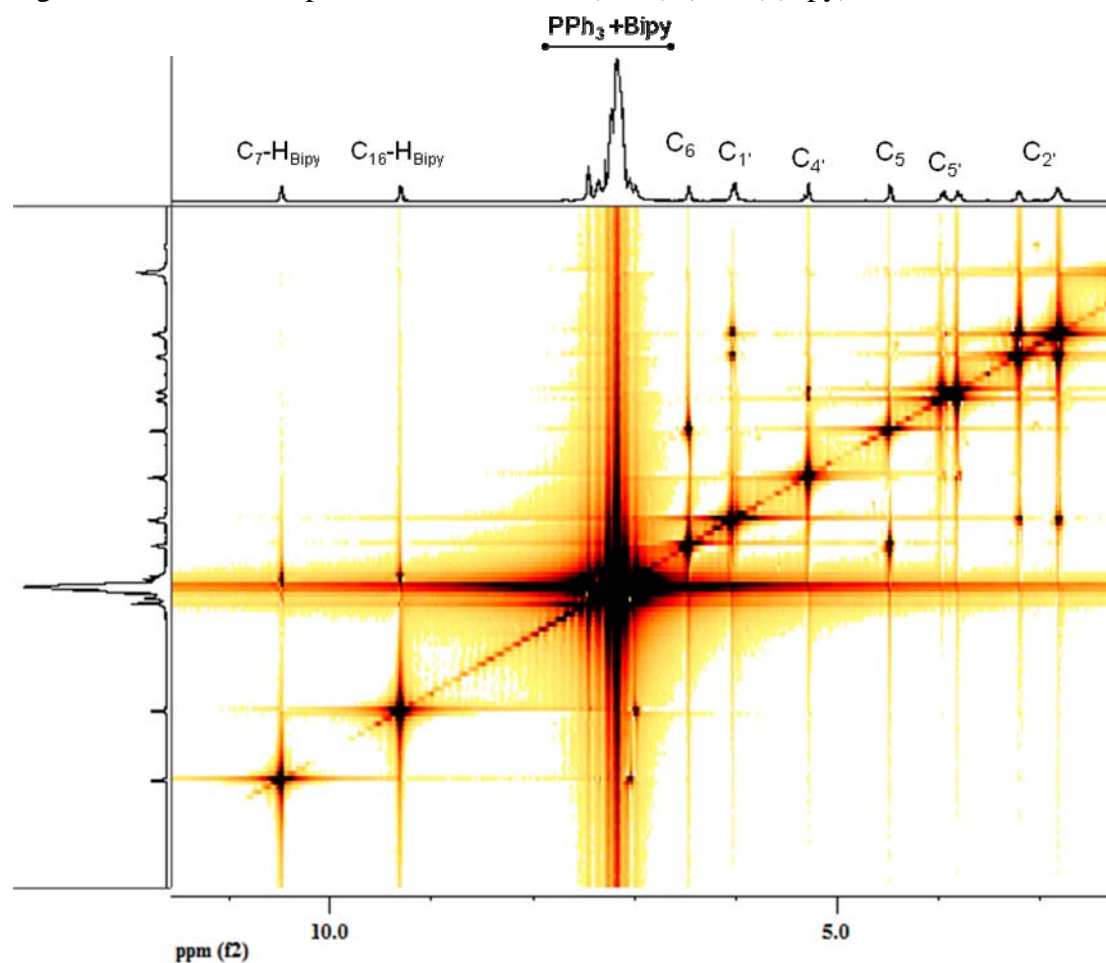


Figure S10 - 2D [^1H , ^1H]-COSY spectrum for *trans*-[Ru(PPh₃)₂(3TC)(bipy)]ClO₄, in CDCl₃.

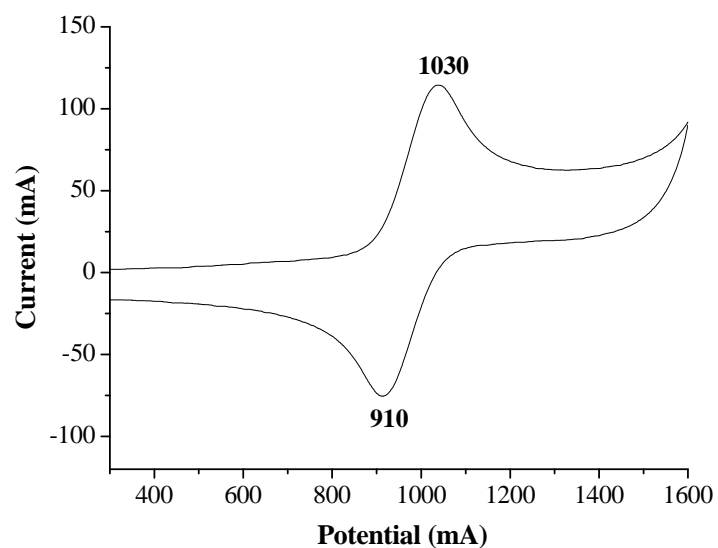


Figure S11 - Cyclic voltammetry for $[\text{Ru}(\text{PPh}_3)_2(3\text{TC})(\text{bipy})]\text{ClO}_4$, $1.0 \times 10^{-3} \text{ molL}^{-1}$ in CH_2Cl_2 with 0.1 molL^{-1} of NBu_4ClO_4 , scan rate 100 mVs^{-1} , measured at a platinum electrode.

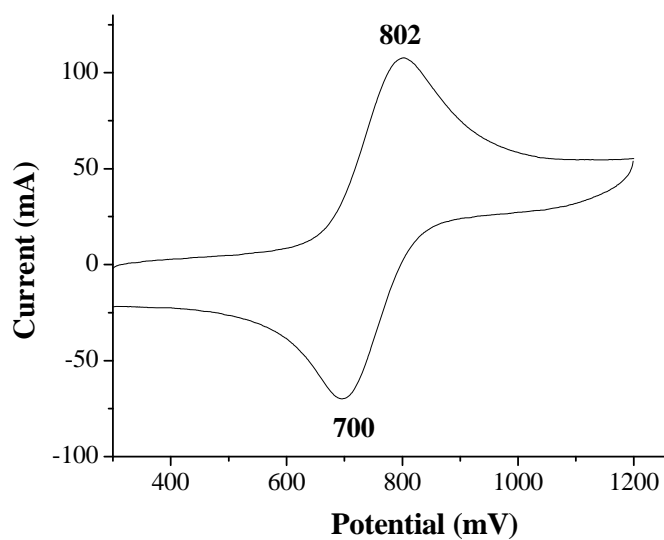


Figure S12 - Cyclic voltammetry for $[\text{Ru}(\text{PPh}_3)_2(\text{CYD})(\text{bipy})]\text{ClO}_4$, $1.0 \times 10^{-3} \text{ molL}^{-1}$ in CH_2Cl_2 with 0.1 molL^{-1} of NBu_4ClO_4 , scan rate 100 mVs^{-1} , measured at a platinum electrode.

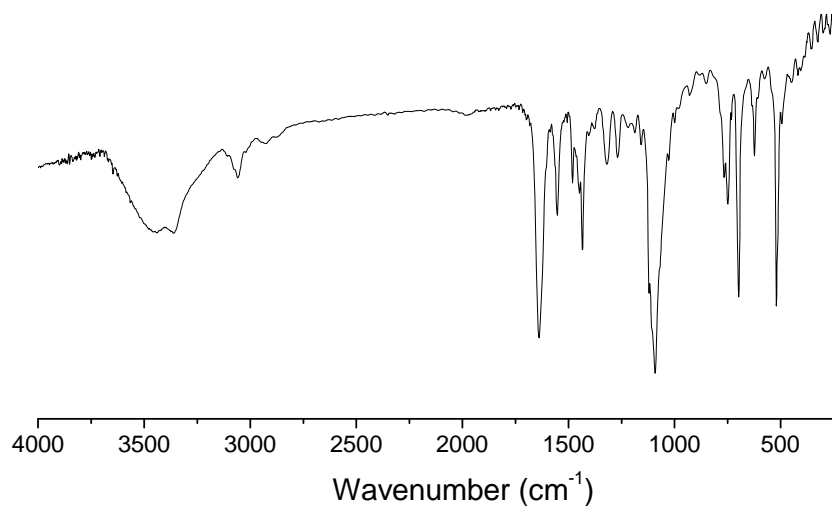


Figure S13 - Infrared spectrum for $[\text{Ru}(\text{PPh}_3)_2(3\text{TC})(\text{bipy})]\text{ClO}_4$, in KBr pallets.

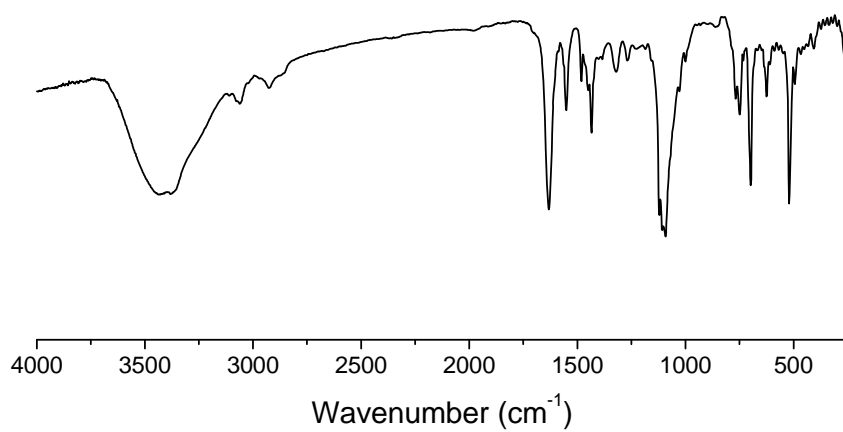


Figure S14 - Infrared spectrum for $[\text{Ru}(\text{PPh}_3)_2(\text{CYD})(\text{bipy})]\text{ClO}_4$, in KBr pallets.